Individually Frequency Tunable Dual- and Triple-band Filters in a Single Cavity

SAI-WAI WONG[1], (Senior Member, IEEE), FEI DENG[2], (Student Member, IEEE), YU-MING WU[2], JING-YU LIN[2], (Student Member, IEEE), LEI ZHU[3], (Fellow, IEEE), QING-XIN CHU[2], (Senior Member, IEEE), AND YANG YANG[4], (Member, IEEE)

[1]College of Information Engineering, Shenzhen University, Shenzhen 518060, China
[2]School of Electronic and Information Engineering, South China University of Technology, Guangzhou 510640, China
[3]Department of Electrical and Computer Engineering, Faculty of Science and Technology, University of Macau, Macau 999078, China
[4]School of Computing and Communications, University of Technology Sydney, Ultimo, NSW 2007, Australia

Corresponding author: Sai-Wai Wong (wongsaiwai@ieee.org)

ABSTRACT This paper presents a new class of second-order individually and continuously tunable dual- and triple-band bandpass filters in a single metal cavity. Each passband is realized by two identical metal posts. These dual- and triple-band tunable filters are achieved by putting two or three identical sets of metal-post pair in a single metal cavity. Metal screws are co-designed as a part of the metal posts to control their insertion depth inside the cavity. In this way, the resonant frequencies can be continuously controlled and designed at the desired frequency bands. Moreover, the distance between the two metal posts in a post pair can be freely tuned. Thus, the external quality factor (Q_e) and coupling coefficient (k) between the adjacent modes can be easily adjusted to meet the specified requirement in synthesis design. At the bottom of the cavity, some grooves are used to extend the tunable frequency range and make the resonant frequency linearly varied with the height of the metal post. The center frequency of each passband can be independently tuned with a frequency range of 0.8–3.2 GHz and tunable ratio of 4. Finally, the continuously tunable dual- and triple-band bandpass filters prototypes with second order response are designed and fabricated, of which each passband can be individually tuned with a large tuning range.

INDEX TERMS Tunable bandpass filter, dual- and triple-band, individual tunable cavity filter, single cavity, groove.

I. INTRODUCTION

Microwave filters are one of indispensable components in many types of radio frequency (RF) communication, radar and spectrum measurement systems. In particular, cavity filters are widely used in the base station of wireless communication systems due to their inherently adopted high power handling capacity and low in-band insertion loss [1]. With the rapid development of multiple services in recent years, the usage of multiple frequency bands has triggered the demand for multiple-band filters. Recently, some multiple-band filters [2]–[7] have been reported with the capability of performance enhancement in wireless communication systems, where the multi-channel services front-ends are expected. In communication systems, reconfigurable or tunable filters are one of the most essential microwave components due to the merits of reconfigurability and multifunction

capability. In recent years, many types of tunable bandpass filters have been proposed using different tuning devices, such as MEMS [8]–[11], varactors [12]–[14], mechanical tuners [15]–[17] and ferrite-loaded [18]. In general, MEMS devices have a large insertion loss but fast tuning speed. Varactors have a better insertion loss than MEMS but the tuning range is relatively narrow. By mechanically adjusting the positions of the capacitive components of the tuner, mechanical tuning devices in cavity filters can achieve small insertion loss. However, this method has the challenges from device miniaturization and sensitive passband performance due to the critically specified coupling coefficients. As a desirable performance, flexible passband tunability turns to be an attractive feature in modern communication systems due to its potential benefits in size and cost reduction at system level by replacing multiple filters using one.

It is a common technology by using a planar integrated structure to build up these multiple-band tunable or reconfigurable filters [19]–[24]. However, in general, the planar multiple-band tunable filters present two drawbacks: large insertion losses and narrow tunable frequency range. As discussed in [19]–[24], the in-band insertion loss of these tunable filters are usually larger than 3 dB. In particular, the work in [24] shows that its insertion loss is as large as 7 dB in the tunable frequency range. Undoubtedly, the desirable performance of wide frequency tuning range and multiple-band ability is quite challenging by using planar structure due to the inherent limitation as a 2-dimensional structure. The reported literature reveals that the highest and lowest tunable frequency range ratio (f_H/f_L) of a tunable multiple-band planar filter is usually smaller than 2.0 [23], [24]. To achieve a wider tuning range, it is expected to effectively control the intra-resonator coupling [19]. However, it is difficult to control the coupling coefficient (k) during the process of frequency tuning because of the restricted freedom of structural movement of the filter.

Therefore, a novel and efficient inner-resonator coupling technique is needed for multiple passband filters with wide tuning range without deteriorating effect on the passband performance over the entire tuning frequency range.

In this paper, we present a new approach of designing the individually and continuously tunable cavity bandpass filters for dual- and triple-band applications. The proposed multiple-band tunable filters have a wide tuning frequency range from 0.8 to 3.2 GHz with a tuning ratio f_H/f_L of 4. Within the tunable frequency range, the intra-resonator coupling coefficient (k) can be effectively controlled by freely tuning the distance between the two metal posts in a post pair. As a highlight of this design, each passband can be controlled independently without affecting its neighboring passband(s). Notably, all the resonators are designed in a single metal cavity without using additional coupling windows, metallic walls or coupling screws in between neighboring resonators, leading to a very simple tuning mechanism. To verify the proposed design approach and predicted the frequency responses, two prototypes of dual- and triple-band tunable filters are designed, fabricated and measured. The measured results demonstrate the individually and continuously tuning capability of the dual- and triple-band cavity filters in a wide frequency range.

II. CONTINUOUSLY TUNABLE SINGLE-BAND FILTER
This section introduces a single resonator with three types of configured resonant cavities. The proposed resonator is selected based on the comparative studies, which is used as a basic unit for single band bandpass filter design. All filter simulations are used CST.

A. WIDE TUNING RANGE OF COAXIAL RESONATOR
Fig. 1(a) depicts the basic configuration of a coaxial cavity resonator. It consists of one resonant metallic post with diameter $D_2 = 4$ mm, which is loaded with a thin disc at its bottom
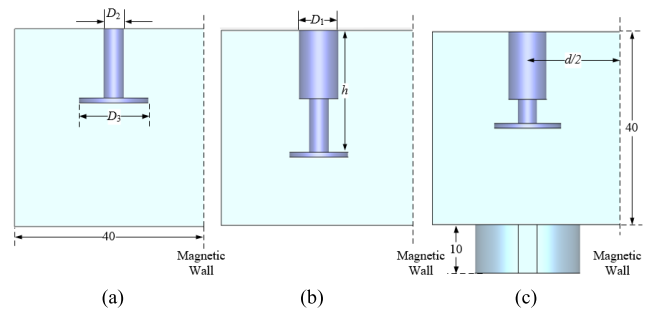

FIGURE 1. Configuration of the proposed three types of resonant cavities. (a) Case-A: resonant posts with $D_2 = 4$, $D_3 = 7$. (b) Case-B: added metal sleeves with $D_1 = 8$ and $h = 14$ in length. (c) Case-C: added grooves. All in mm.

to produce an extra capacitance value, namely, Case-A. The principle of frequency tuning in Case-A can be easily understood by following explanation. According to the capacitance equation $C = \varepsilon * Area/distance$, the capacitance C is inversely proprotional to the distance between the disc and the bottom of the cavity. Thus, the resonant frequency can be tuned by the insertion depth of the posts, namely h in Case-A. When the parameter D_2 is selected as 4.0 mm, the resonant frequency of Case-A varies as a function of h as displayed by the black-rhombus curve in Fig. 2. When the disc is moved far away from the bottom metellic wall, the capacitance value becomes too weak to dominate the resonant frequency. In contrast, the inductance component of the resonant mode becomes much influential to resonant frequency. According to (1) from [25], the inductance value per unit length depends on the ratio of r_2/r_1, where r_1 and r_2 are the inner and outer conductor radii of a coaxial resonator. Obviously, a high resonant frequency can be obtained by decreasing the ratio of r_2/r_1. Hence, a large diameter sleeve with $D_1 = 8$ mm is embedded in the top wall, as shown in Fig. 1(b), namely, Case-B. The simulated results of the resonant frequency against h are plotted by the red-triangle curve in Fig. 2. Compared with Case-A in Fig. 2, Case-B is found to achieve a wider tuning frequency. Thus, the tuning frequency range can be expanded by embedding these sleeves in the resonant post.

$$L \propto \left(ln\frac{r_2}{r_1} + \frac{1}{4} \right) \qquad (1)$$

In order to achieve a better tuning capability in practical application, a cylindrical groove is implemented under the resonant post to improve the linearity of frequency-tuning curve, namely, Case-C. Fig. 1(c) shows the designed groove engineered at the bottom of the cavity which has the same dimensions as Case-B. As shown in Fig. 2, the lower band frequency is less sensitive in Case-C than the other two cases. The reason is that in case- B when the disc is very close to the bottom metallic wall, the distance between the two metal faces is very small leading to a large variation of capacitance value when h is slightly changed. With the groove, the capacitance is produced by both the edge of the disc and the edge of the groove. This edge-to-edge capacitance is less sensitive
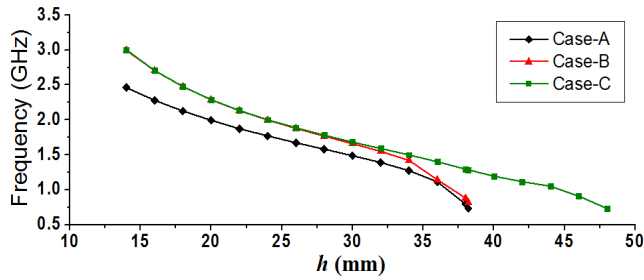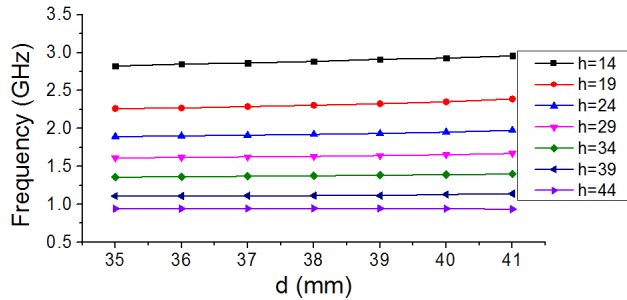
FIGURE 2. Resonant frequency as a function of *h*.

FIGURE 3. Resonant frequency versus *d* under different *h* (mm).

to the face-to-face capacitance. For this reason, the edge-to-edge capacitance provides a smooth transition before the disc reaches the bottom of the metallic wall. Thus, the variation of the capacitance in terms of *h* is less sensitive using the proposed groove. The parameter *d* is designed to control the intra-coupling and the external quality factor. From Fig. 3, the resonant frequency is almost unchanged throughout the entire frequency-tuning band (with less than 0.4% variation) when the distance *d* tunes from 37 to 41 mm. This shows that the parameter *d* has almost no impact on resonant frequency.

B. SINGLE-BAND TUNABLE FILTER AND SIMULATED RESULTS

Fig. 4 shows the structure of a tunable single-band bandpass filter with a second order filter response. To meet the demand in good tunable filtering performance, an appropriate feeding method becomes critical to achieve a wide frequency tuning range. Three methods have been commonly used to design
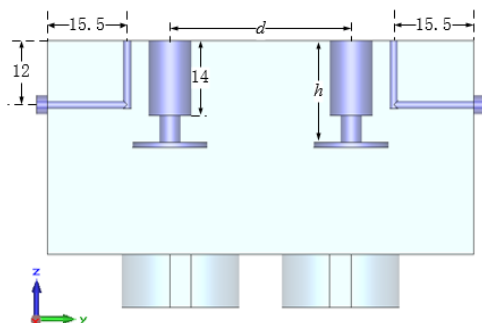
the input/output coupling structure in a coaxial cavity filter, namely, direct coupling, loop coupling and disc capacitive coupling. The direct coupling arouses the strongest coupling, but the probes need to be physically contacted with the resonant posts, which is difficult to be applied in this scenario as the resonator posts are moving during the tuning process. The disc capacitive coupling brings out the weakest coupling among these three methods. It cannot support a wide frequency tuning range. The loop coupling can not only support a wide frequency tuning range, but also provide a strong coupling from input/output ports without a physical contact on the tuning posts. Therefore, the loop coupling is used as the input/output structure in the design of this tunable filter. As shown in Fig. 4, two ports are placed in the symmetrical sidewall of the metal cavity through a standard 50 ohm coaxial line as a feeder. Two L-shaped conductors of the probes are extended into the cavity as the magnetic coupling probes for excitation of the resonant modes. One end of the L-shaped conductor is shorted to the top wall of the metal cavity, while the other end is connected to the input/output port. In order to have enough space to tune the distance between the two metal posts in a post pair, the height and length of L-shaped conductor are set as 12.0 mm and 15.5 mm, respectively, to provide sufficient input/output coupling to the first resonator. Once the probes are fixed, *d* can be freely changed by tuning the posts within a sliding slot. In practice, there is a screw in each post for vertically tuning of the disc.
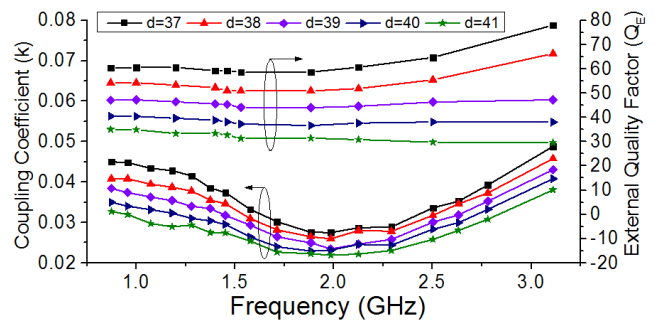

FIGURE 5. Variation of coupling coefficient (*k*) and external quality factor (*Q_E*) as a function of *h* under different *d*. All in mm.

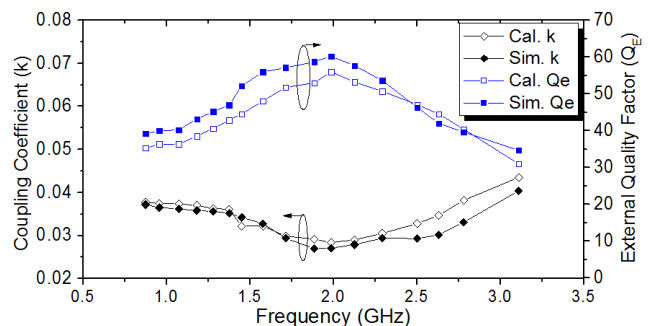**FIGURE 4.** Structure of tunable single-band filter. All in mm.

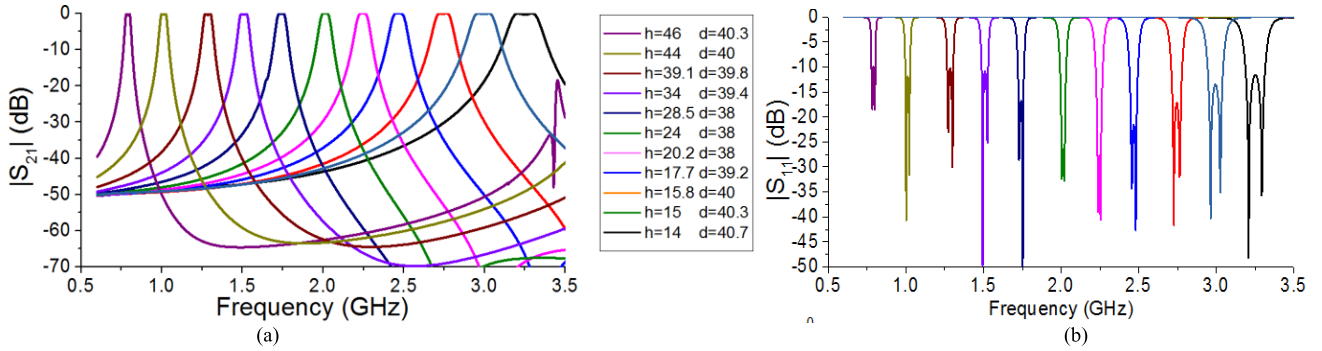**FIGURE 6.** Calculated and Simulated *k* and *Q_E* over tuning range.

FIGURE 7. Simulated results of the proposed continuously tunable single-band filter under different tuned frequencies. (a) $|S_{21}|$ and (b) $|S_{11}|$.

After designing the input/output coupling structure, the study of the coupling coefficient (k) and the external quality factor (Q_E) is the next critical task for achieving the desired filter performance. During the process of frequency tuning, the controllable intra-resonator coupling is important to achieve a good passband. In this work, the coupling coefficient (k) is determined by the distance d between the two resonant posts. The variation of coupling coefficient as a function of frequency under different d is plotted in Fig. 5. It can be seen that the intra-resonant coupling becomes stronger with a reduced d. Thus, a mechanism of controlling the coupling coefficient (k) is realized by moving the position of the two resonant posts. Because the magnetic coupling turns to the electric coupling at the frequency around 2 GHz, the k values appear a decreasing and an increasing tendency before and after 2 GHz. Fig. 5 also plots the external quality factors, Q_E, against the frequency under various d (Note: the resonant frequency is directly related to h as shown in Fig.2). The curves show that, when the frequency is tuning, Q_E is stable with $d = 37$, 38 and 39 mm. In contrast, when d is set to be more than 40 mm and the frequency is higher than 2.2 GHz, Q_E has larger variation. Thus, when the tunable frequency is tuned to higher than 2.2 GHz, d should not be larger than 40 mm because of unstable Q_E. In addition, Q_E reduces with the increment of d. This inspires us that we can compensate for the variation of Q_E by changing the d during the tuning process. This can be done by moving the posts within the sliding slot along the y-axis. Furthermore, the distance d can be employed to control the coupling between two resonators. Thus, by appropriately tuning the d and h, two resonant frequencies can form a passband in the desired frequency range.

$$Q_E = \frac{g_0 g_1}{FBW} \tag{2}$$

$$k = \frac{FBW}{\sqrt{g_1 g_2}} \tag{3}$$

We all know that if the realized k and Q_E satisfy the element values of the filter synthesis method, a good passband will be formed. According to (2) and (3) from [26], a fractional bandwidth more than 3.3% and a passband ripple between 0.2 and 0.5 dB are chosen for theoretical calculations of k and Q_E, of which the frequency response curves
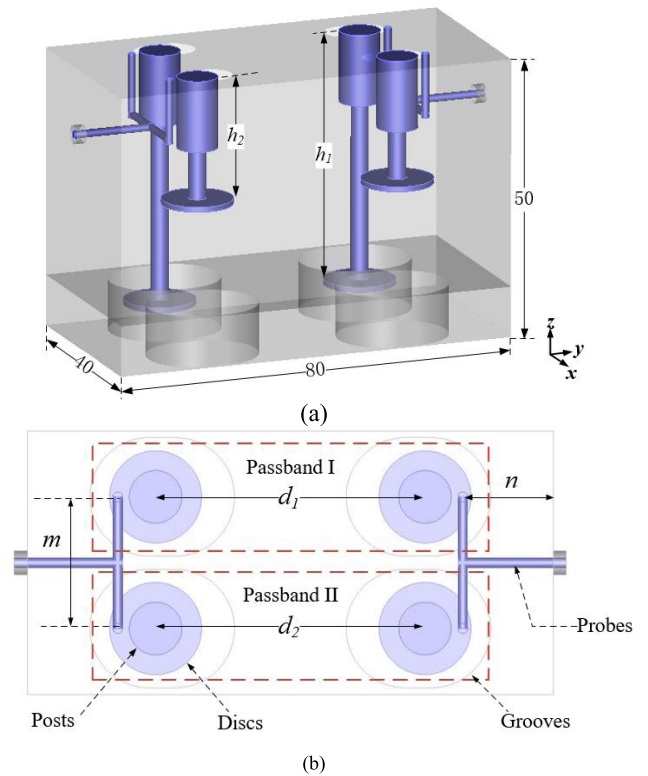

FIGURE 8. Configuration of the individual continuously tunable dual-band filter. (a) 3D-view. (b) Top-view. All in mm.

are plotted in Fig. 6. The extracted values of the simulated k and Q_E from the circuit model are also plotted in Fig. 6 for comparison. The two sets of curves are reasonably matched over the entire frequency tuning band. This shows that the passbands of our proposed tunable filter satisfy the filter synthesis method over the entire frequency band. Thus, Fig. 6 can be used as the design guidelines to determine the values of d and h with satisfactory passband performance.

The basic design procedure has been summarized as the following:

- Step 1: If the passband frequency is determined, according to Fig. 2, the value of h is determined. For example, a passband is designed at 2 GHz, $h = 24$ mm must be chosen from Fig. 2.
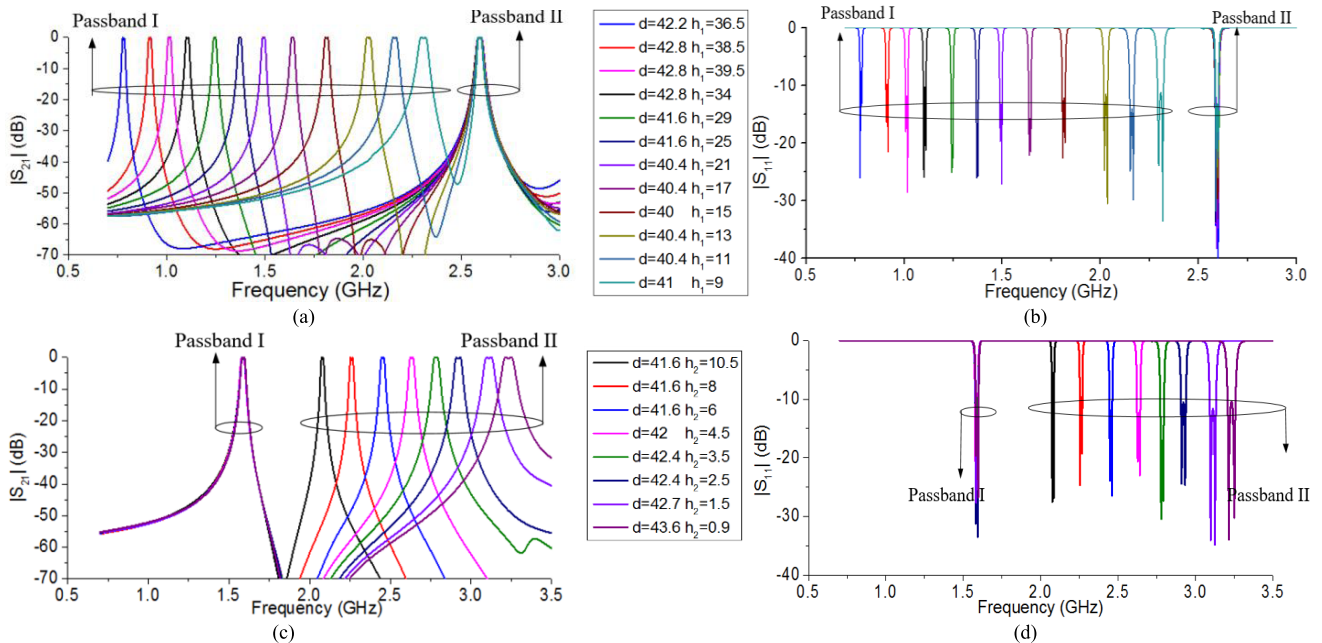
FIGURE 9. Simulated results for demonstration of tuning performance, (a) tuning of $|S_{21}|$ with fixed Passband II, (b) tuning of $|S_{11}|$ with fixed Passband II, (c) tuning of $|S_{21}|$ with fixed Passband I, (d) tuning of $|S_{11}|$ with fixed Passband I.

- Step 2: Find the calculated k and Q_E from Fig. 6 according to the chosen frequency, e.g. at 2 GHz, k is 0.026 and Q_E is 55 from Fig. 6.
- Step 3: Find the value of d in Fig. 5 according to the chosen value of k and Q_E in Step 2, e.g. $k = 0.026$, and $Q_E = 55.2$ at 2 GHz, the $d = 38$ mm is determined in Fig. 5.

Following the steps above, a second order bandpass filter response can be realized throughout the entire frequency band with the particular value of d from Fig. 5. Fig. 7 shows the simulated S-parameters of a continuously tunable single-band cavity filter. The example, demonstrated in Steps 1-3, with the passband center frequency at 2 GHz is marked in Fig. 7(a). A good passband is formed with $h = 24$ mm and $d = 38$ mm in the circuit model. This example proves that the method proposed is useful to design a good passband within the proposed frequency range. The filter can be continuously tuned from 0.8 GHz to as high as 3.2 GHz with a 3-dB fractional bandwidth (FBW) of 4.5±1.2%, and an unloaded Q value varies from 4250 to 6527. Meanwhile, it is seen that the return loss is better than 10 dB and the insertion loss is less than 0.3 dB. Particularly, there is only a single passband over the entire tuning frequency range without the emergence of any parasitic passband in the upper-band. Taking the advantage of the grooves, the process of tuning becomes more accurate and linear.

III. TUNABLE DUAL- AND TRIPLE-BAND CAVITY FILTERS
A. DUAL-BAND FILTER
In this section, the individually and continuously tunable dual- and triple-band cavity filters are presented based on

Section II. All the components are employed in a single cavity. Figs. 8(a) and 8(b) show the physical configuration of 3-D view and top-view of the tunable dual-band cavity filter, respectively. There is no coupling window and no intra-
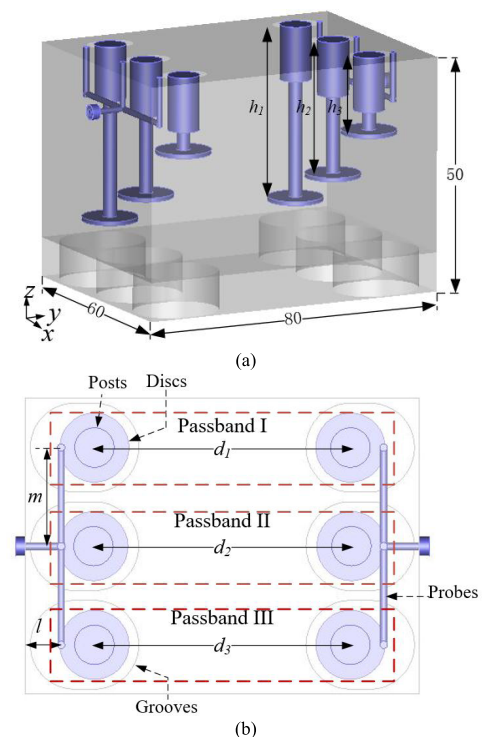

FIGURE 10. Configuration of the individual continuously tunable triple-band filter. (a) 3D- view. (b) Top-view. The parameters are: $m = 20$, and $l = 7$. All in mm.
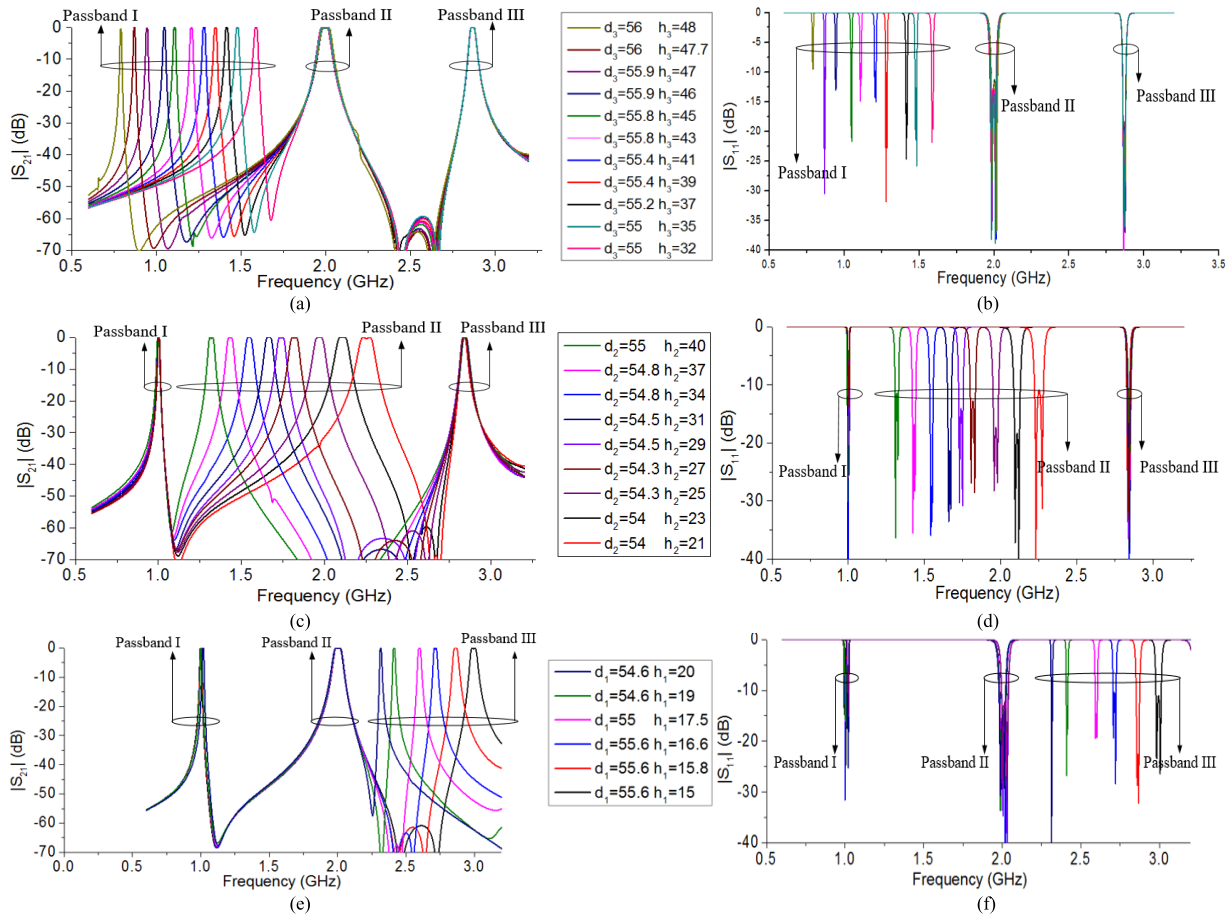
FIGURE 11. Simulated *S*-parameter with tuning performance, (a) tuning of $|S_{21}|$ with fixed Passband I and II, (b) tuning of $|S_{11}|$ with fixed Passband I and II, (c) tuning of $|S_{21}|$ with fixed Passband I and III, (d) tuning of $|S_{11}|$ with fixed Passband I and III, (e) tuning of $|S_{21}|$ with fixed Passband II and III, (f) tuning of $|S_{11}|$ with fixed Passband II and III.

cavity metallic wall inside the cavity. Fig. 8(b) indicates two post pairs (each pair contains two metal posts) corresponding to two independently and continuously tunable passbands inside a single cavity, namely, Passband I and Passband II.

In order to achieve the function of individual tuning, the intra cavity coupling between two frequency bands must be small enough, which requires a certain distance between the post pairs. However, the dimension of the cavity needs to be as small as possible for miniaturization purpose. Considering the tradeoff between the isolation and size of the filter, the distance *m* is selected as $\lambda/4$ with respect to the upper-frequency band 3.2 GHz. Based on the design of a single-band filter, $n = 15.5$ mm is selected. As shown in Figs. 8(a) and 8(b), the insertion depth of the posts (h_1 and h_2) of the Passband I and Passband II can be differently selected to achieve different resonant frequencies and perform dual-band behavior. It is obvious that the structure is symmetrical in the *x-z* plane for both Passband I and Passband II structure. For example, the posts, discs and sliding windows are identical along the symmetrical x-z plane. In addition, four identical grooves are employed under the metallic discs, and their depths are all selected to be 10 mm. A T-shaped feeding structure is used to provide
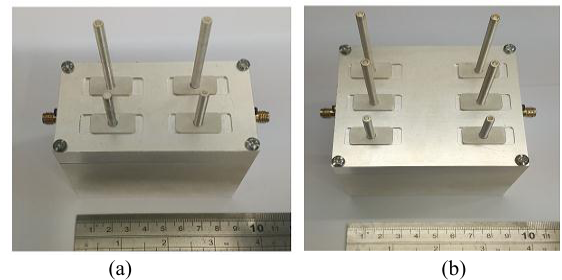
FIGURE 12. External photography of the proposed tunable filters, (a) the dual-band filter, (b) the triple-band filter.

two coupling paths to Passband I and Passband II structures with $n = 15.5$ mm and the center-to-center distance between Passband I and Passband II structures is selected to be $m = 20$ mm.

The tuning mechanism of this dual-band filter is similar to that of its single-band counterpart as discussed in Section II. To demonstrate the continuously individual-tuning capability of this dual-band filter, we fix one passband at an arbitrary chosen frequency and tune the frequency of other passband. Fig. 9 indicates the simulated results of the dual-band tunable
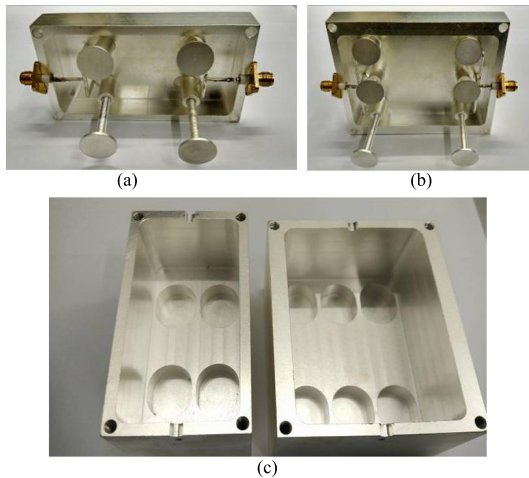
FIGURE 13. Internal photography of the proposed tunable filter, (a) top-cover of the dual-band filter, (b) top-cover of the triple-band filter, (c) bottom cavity of the dual-band filter (left) and bottom cavity of the triple-band filter (right).

filter. We tune the length of two posts to change the passband frequency and adjust the two posts along the sliding slots to control the value of Q_E and k to perform a required passband performance. Fig. 8(a) shows that when we fixed Passband II at 2.59 GHz with $h_2 = 19$ mm and $d_2 = 42.2$ mm, Passband I can be continuously tuned from 0.78 to 2.3 GHz by changing h_1 from 21 to 43.5 mm and d_1 from 40 to 42.8 mm. The fractional bandwidth (FBW) of Passband I varies from 1.25% to 2%. Fig. 9(c) illustrates that when Passband I is fixed at 1.58 GHz with $h_1 = 34.2$ mm and $d_1 = 41.6$ mm, Passband II exhibits a tuning frequency range from 2 to 3.24 GHz with h_2 tuned from 14.9 to 24.5 mm and

d_2 tuned from 41.0 to 43.6 mm. The FBW varies from 0.8% to 2.3%. It is noteworthy that the tuning elements of Passband I and Passband II are identical and they can be tuned in the entire frequency range from 0.8 GHz to 3.2 GHz. In this case, the unloaded Q of dual-band filter varies from 2751 to 3562.

B. TRIPLE-BAND FILTER
The final configuration of the individually and continuously tunable triple-band filter is depicted in Figs. 10(a) and 10(b). Again, the three sets of tuning elements of the triple-band filter are identical. In order to achieve a triple-band performance, the size of the cavity needs to be larger than previous tunable single- and dual-band cavity filters. Its volume becomes 80 mm × 60 mm × 50 mm. Next, the number of resonators needs to be properly modified for accommodating three identical pairs of metal posts. Meanwhile, each of input/output feeding networks in the triple-band filter has three branches instead of two in contrast to the dual-band filter. The distance m between the neighboring post pairs of the proposed filter is set as 20 mm, and the length of feeding structure l is set as 7 mm. Fig. 11 plots the simulated results of continuously individual-tunable triple-band filter. For clear demonstration, three tuning cases are displayed in Fig. 11 to verify the individually and continuously tuning capability. Fig. 11(a) shows that, when Passband II and Passband III are fixed at 2 and 2.8 GHz with $h_2 = 23.75$ mm, $h_3 = 43$ mm, $d_2 = 53.4$ mm and $d_3 = 54$ mm, Passband I can be tuned continuously from 0.8 to 1.65 GHz corresponding to a tuning h_1 from 15.57 to 19.0 mm. Fig. 11(c) shows that the center frequencies of Passband I and Passband III are fixed at 1.1 and 2.8 GHz, respectively, with $h_1 = 46.4$ mm, $h_3 = 16$ mm, $d_1 = 54.6$ mm and $d_3 = 54.6$ mm.
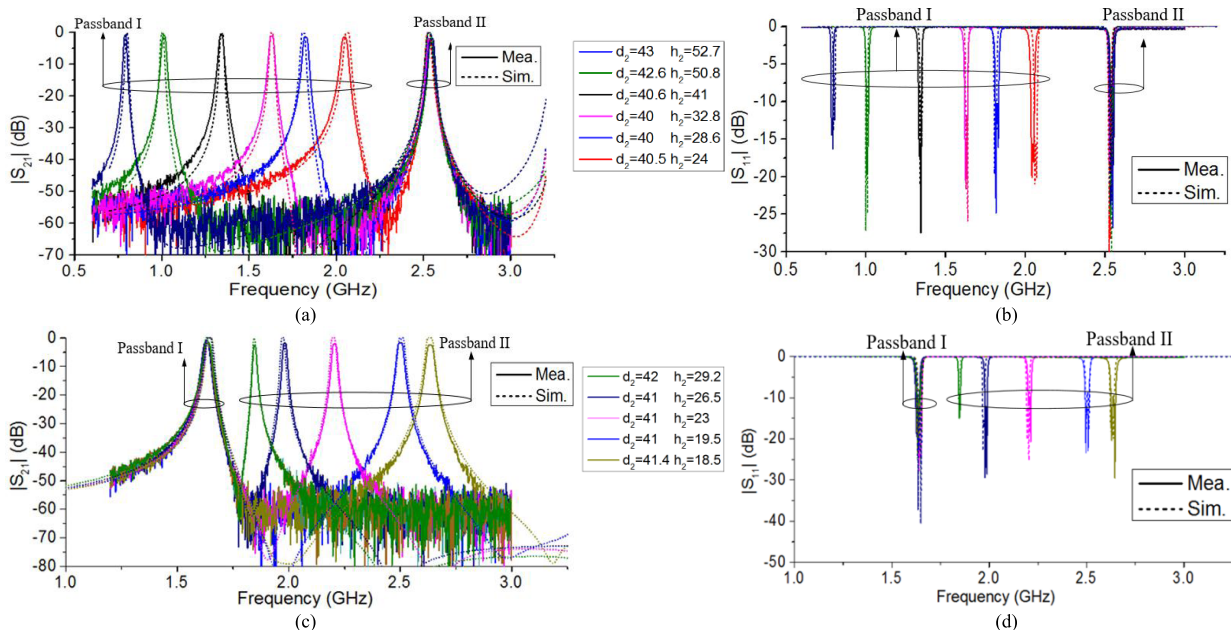

FIGURE 14. Measured S-parameter of the individually and continuously tunable dual-band filter, (a) tuning of $|S_{21}|$ with fixed Passband II, (b) tuning of $|S_{11}|$ with fixed Passband II, (c) tuning of $|S_{21}|$ with fixed Passband I, (d) tuning of $|S_{11}|$ with fixed Passband I.

TABLE 1. Comparison among tunable cavity filters.

	Tunable range (GHz)			Number of Passband	Tuning ratio	Size (λ_c^2/λ_c^3)	Controllable intra-coupling	IL (dB)	Tuning device
	f_1	f_2	f_3						
[6]	0.9	1.8	N.A.	2	N.A.	0.416*0.13.3*0.239	No	1-1.9	N.A.
[11]	4.07-5.58	N.A.	N.A.	1	1.37	0.152*0.152*0.152	No	3.2-4.9	MEMS
[14]	1.15-1.74	2.24-3.64	N.A.	2	1.65	0.15*0.115 (planar)	No	1.1-7.5	Varactors
[18]	0.37-1.03	N.A.	N.A.	1	2.76	0.56*0.22 *0.22	No	0.1-0.3	Ferrite Loaded
[23]	1.48-1.8	2.48-2.88	N.A.	2	1.21	0.25*0.25 (planar)	Yes	2.8-4.8	Varactors
[24]	1.1-1.7	2.04-2.4	N.A.	2	1.7	0.173*0.092 (planar)	No	6.4-11	Varactors
This work	0.8-3.2	0.8-3.2	0.8-3.2	3	4	0.21*0.16*0.133	Yes	0.6-2.6	Screws

λ_c: The wavelength at the center frequency of the tuning frequency range. IL: Insertion loss.
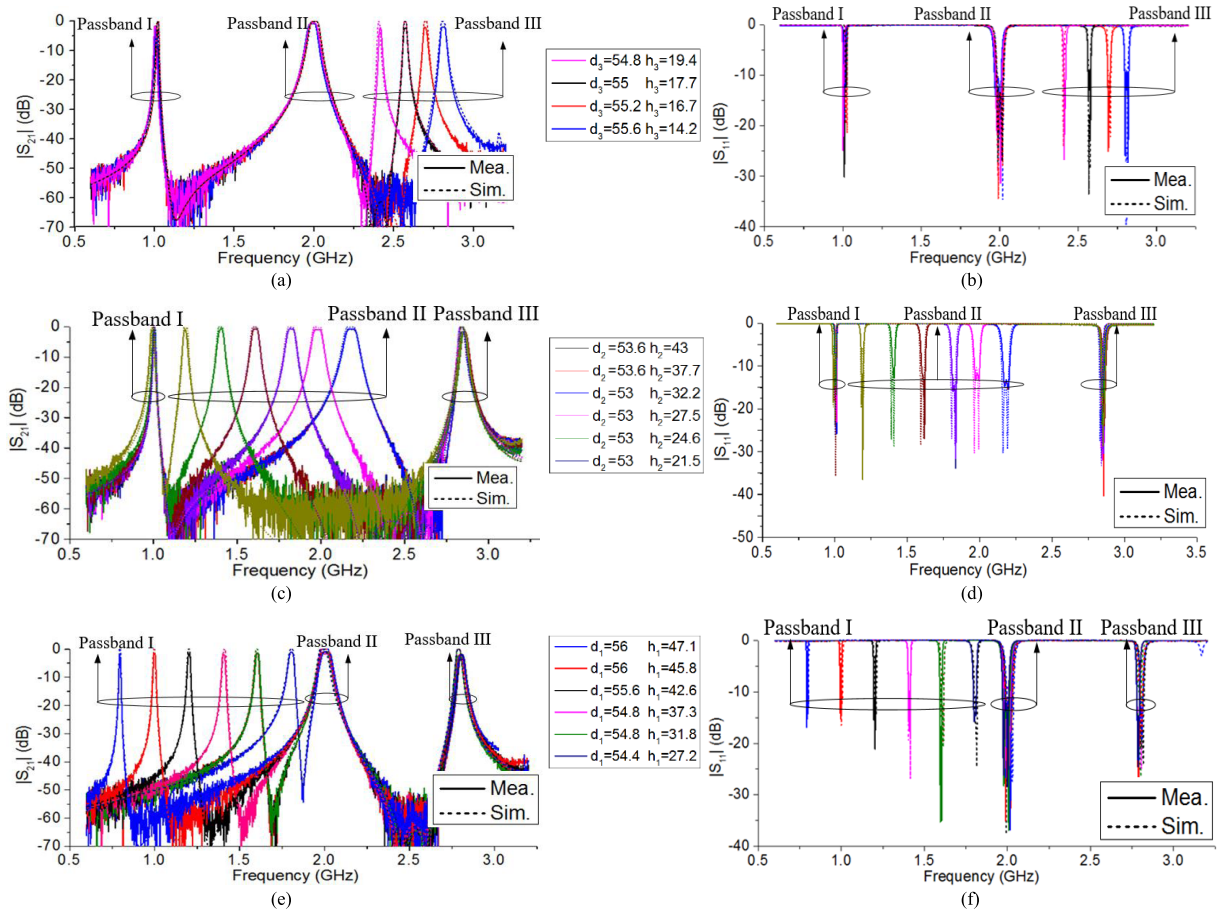

FIGURE 15. Measured *S*-parameters of the individually and continuously tunable triple-band filter, (a) tuning of $|S_{21}|$ with fixed Passband I and II, (b) tuning of S_{11} with fixed Passband I and II, (c) tuning of $|S_{21}|$ with fixed Passband I and III, (d) tuning of $|S_{11}|$ with fixed Passband I and III, (e) tuning of $|S_{21}|$ with fixed Passband II and III, (f) tuning of $|S_{11}|$ with fixed Passband II and III.

Passband II can be tuned from 1.2 to 2.3? GHz with h_2 being tuned from 5 to 26 mm. Fig. 11(e) shows that, when Passband I and Passband II are fixed at 1 and 2 GHz with their tunable parameters $h_1 = 46.4$ mm, $h_2 = 24.3$ mm, $d_1 = 54.6$ mm and $d_2 = 53.4$ mm, the Passband III can be individually tuned from 2.4 to 3 GHz corresponding to a varying h_3 from 14 to 20 mm. As shown in Figs. 11(b), (d) and (f), the designed filters have the return loss better than –10 dB for all the passbands, which implies a good impedance matching. Meanwhile, the unloaded quality factor Q is obtained from 2000 to 3151.

IV. EXPERIMENTAL RESULTS

Following the discussion in Sections II and III, two individually and continuously tunable dual- and triple-band filters are fabricated and measured. Figs. 12(a) and 12(b) shows components, the fabricated filter cavity is divided into the two detached parts: the top-cover and the bottom cavities. Figs. 13(a) external view of the photography of dual- and triple-band filters, respectively. In order to facilitate the assembly of tuning and 13(b) shows the top-cover internal view of dual- and triple-band filters, respectively. Fig. 13(c) shows the bottom cavity internal view of the two filters. All

of the components and the filter cavities are silver-plated to maintain a low the in-band insertion loss from the metal. The top cover of the filter cavity has slots embedded for sliding the posts horizontally. For structural support of the tunable posts, metal plates are implemented on the top surface of the sliding slots of the tunable posts.

In Fig. 14, there is a good agreement between the simulated and measured results of tunable dual-band filter. Fig. 14(a) shows the results in the case that the Passband II is fixed and the Passband I is tuned. The return loss is better than 10 dB in the tuning frequency passbands as shown in Fig. 14 (b). Fig. 14(c) displays the results in the case that the Passband I is fixed and the Passband II is tuning. The return loss in Fig. 14(d) is better than 10 dB in the tunable frequency passbands. This satisfies with the results in Fig. 9 and experimentally proves the continuously and individually tuning capability of the proposed dual-band cavity filter over a wide frequency range. From the simulated results, the proposed filters are designed to have the in-band insertion loss less than 0.5 dB. But the measured insertion loss varies from 0.86 dB to 2.7 dB over tuning range. The difference between the simulated and measured results is mainly due to the screws-based mechanical tuning approach. The non-ideal contact between the tuning screws and the conductors may result in extra insertion losses. Due to the limitation of metal fabrication, the thread cannot cover the entire body of the screw leading to a shortened the tuning range (0.8 to 2.6 GHz) in measurement, which is about 600 MHz shorter than the simulated one. Fig. 15 shows three sets of simulated and measured results of the triple-band filter: 1) Set One, Fig. 15(a) and (b), the Passband I and II are fixed, while the Passband III is tuning, 2) Set Two, Fig. 15(c) and (d), the Passband I and III are fixed, while the Passband II is tuning, 3) Set Three, Fig. 15(e) and (f), the Passband II and III are fixed, while the Passband I is tuning. This experiment proves that the proposed triple-band filter can achieve individually and continuously frequency-tuning capability over a wide frequency range. Meanwhile, the triple-band filter provides better than 10 dB return loss as illustrated in Figs. 15(b), (d), and (f). The simulated and the measured results agree well with each other in FBW. Similar to the case in dual-band filter, the measured frequency-tuning range covers 0.8 to 2.8 GHz, which is 400 MHz shorter than the simulated one, due to the limitation of metal screws fabrication. The measured in-band insertion loss varies from 0.6 to 2.6 dB. Table I shows that, among the reported single-band and multi-band freqeuncy-tunable cavity filters, the mechnism generally applied for dual- and triple-band tuanable filters have not yet been reported, according to the authors' knowledge. Compared to those single-band tunable filters, our proposed filter has achieved the highest tuning ratio of 4, almost two times better than the reported ones. Moreover, our filter is very compact comparing with the counterparts, especially for the triple-band case. It is noteworthy that only a single metal cavity is implemented for the realization of the dual- and triple-band filters.

V. CONCLUSIONS AND DISCUSSIONS

In this paper, a class of individually and continuously tunable dual- and triple-band filters have been presented. According to the authors' best knowledge, it is the first time that the mechanical-tuning approach is applied to achieve the dual- and triple-band tunable filters with a tunable ratio of 4. This is almost 2 times better than the reported counterparts. Furthermore, all the components and resonators installed in a single metal cavity without any intra-cavity metallic wall, which significantly reduces the fabrication complexity. As experimentally verified, the proposed approach can be used for multiple-band filter designs with individually and continuously tunable capability over a wide frequency range of 0.8-3.2 GHz.

REFERENCES

[1] R. R. Mansour, "Filter technologies for wireless base stations," *IEEE Microw. Mag.*, vol. 5, no. 1, pp. 68–74, Mar. 2004.

[2] G. Macchiarella and S. Tamiazzo, "Design techniques for dual-passband filters," *IEEE Trans. Microw. Theory Techn.*, vol. 53, no. 11, pp. 3265–3271, Nov. 2005.

[3] S. Sun and L. Zhu, "Compact dual-band microstrip bandpass filter without external feeds," *IEEE Microw. Wireless Compon. Lett.*, vol. 15, no. 10, pp. 644–646, Oct. 2005.

[4] P. Mondal and M. K. Mandal, "Design of dual-band bandpass filters using stub-loaded open-loop resonators," *IEEE Trans. Microw. Theory Techn.*, vol. 56, no. 1, pp. 150–155, Jan. 2008.

[5] J. A. Ruiz-Cruz, M. M. Fahmi, and R. R. Mansour, "Triple-conductor combline resonators for dual-band filters with enhanced guard-band selectivity," *IEEE Trans. Microw. Theory Techn.*, vol. 60, no. 12, pp. 3969–3978, Dec. 2012.

[6] F. C. Chen, J. M. Qiu, S. W. Wong, and Q. X. Chu, "Dual-band coaxial cavity bandpass filter with helical feeding structure and mixed coupling," *IEEE Microw. Wireless Compon. Lett.*, vol. 25, no. 1, pp. 31–33, Jan. 2015.

[7] R. Gómez-García and A. C. Guyette, "Reconfigurable multi-band microwave filters," *IEEE Trans. Microw. Theory Techn.*, vol. 63, no. 4, pp. 1294–1307, Apr. 2015.

[8] W. D. Yan and R. R. Mansour, "Tunable dielectric resonator bandpass filter with embedded MEMS tuning elements," *IEEE Trans. Microw. Theory Techn.*, vol. 55, no. 1, pp. 154–160, Jan. 2007.

[9] K. Entesari and G. M. Rebeiz, "A differential 4-bit 6.5–10-GHz RF MEMS tunable filter," *IEEE Trans. Microw. Theory Techn.*, vol. 53, no. 3, pp. 1103–1110, Mar. 2005.

[10] A. Pothier *et al.*, "Low-loss 2-bit tunable bandpass filters using MEMS DC contact switches," *IEEE Trans. Microw. Theory Techn.*, vol. 53, no. 1, pp. 354–360, Jan. 2005.

[11] S.-J. Park, I. Reined, C. Patel, and G. M. Rebeiz, "High-*Q* RF-MEMS 4–6-GHz tunable evanescent-mode cavity filter," *IEEE Trans. Microw. Theory Techn.*, vol. 58, no. 2, pp. 381–389, Feb. 2010.

[12] M. Makimoto and M. Sagawa, "Varactor tuned bandpass filters using microstrip-line ring resonators," in *IEEE MTT-S Microw. Symp. Dig.*, May 2001, pp. 411–414.

[13] A. Anand, J. Small, D. Peroulis, and X. Liu, "Theory and design of octave tunable filters with lumped tuning elements," *IEEE Trans. Microw. Theory Techn.*, vol. 61, no. 12, pp. 4353–4364, Dec. 2013.

[14] J. R. Chen, M. D. Benge, A. Anand, H. H. Sigmarsson, and X. Liu, "An evanescent-mode tunable dual-band filter with independently-controlled center frequencies," in *IEEE MTT-S Int. Microw. Symp. Dig.*, vol. 2. May 2016, pp. 1–4.

[15] B. Yassini, M. Yu, and B. Keats, "A *Ka*-band fully tunable cavity filter," *IEEE Trans. Microw. Theory Techn.*, vol. 60, no. 12, pp. 4002–4012, Dec. 2012.

[16] D. Scarbrough, D. Psychogiou, D. Peroulis, and C. Goldsmith, "Low-loss, broadly-tunable cavity filter operating at UHF frequencies," in *IEEE MTT-S Microw. Symp. Dig.*, May 2015, pp. 1–4.

[17] B. Yassini, M. Yu, D. Smith, and S. Kellett, "A *Ku*-band high-*Q* tunable filter with stable tuning response," *IEEE Trans. Microw. Theory Techn.*, vol. 57, no. 12, pp. 2948–2957, Dec. 2009.

[18] Ö. Acar, T. K. Johansen, and V. Zhurbenko, "A high-power low-loss continuously tunable bandpass filter with transversely biased ferrite-loaded coaxial resonators," *IEEE Trans. Microw. Theory Techn.*, vol. 63, no. 10, pp. 3425–3432, Oct. 2015.

[19] Z. H. Chen and Q. X. Chu, "Dual-band reconfigurable bandpass filter with independently controlled passbands and constant absolute bandwidths," *IEEE Microw. Wireless Compon. Lett.*, vol. 26, no. 2, pp. 92–94, Feb. 2016.

[20] X. Huang, L. Zhu, Q. Feng, Q. Xiang, and D. Jia, "Tunable bandpass filter with independently controllable dual passbands," *IEEE Trans. Microw. Theory Techn.*, vol. 61, no. 9, pp. 3200–3208, Sep. 2013.

[21] C.-F. Chen, "A compact reconfigurable microstrip dual-band filter using varactor-tuned stub-loaded stepped-impedance resonators," *IEEE Microw. Wireless Compon. Lett.*, vol. 23, no. 1, pp. 16–18, Jan. 2013.

[22] G. Chaudhary, Y. Jeong, and J. Lim, "Harmonic suppressed dual-band bandpass filters with tunable passbands," *IEEE Trans. Microw. Theory Techn.*, vol. 60, no. 7, pp. 2115–2123, Jul. 2012.

[23] G. Chaudhary, Y. Jeong, and J. Lim, "Dual-band bandpass filter with independently tunable center frequencies and bandwidths," *IEEE Trans. Microw. Theory Techn.*, vol. 61, no. 1, pp. 107–116, Jan. 2013.

[24] T. Yang and G. M. Rebeiz, "Three-pole 1.3–2.4-GHz diplexer and 1.1–2.45-GHz dual-band filter with common resonator topology and flexible tuning capabilities," *IEEE Trans. Microw. Theory Techn.*, vol. 61, no. 10, pp. 3613–3624, Oct. 2013.

[25] M. N. O. Sadiku, *Elements of Electromagnetics*, 3rd ed. Oxford, U.K.: Oxford Univ. Press, 2001.

[26] J.-S. Hong and M. J. Lancaster, *Microstrip Filters for RF/Microwave Applications*. New York, NY USA: Wiley, 2001.
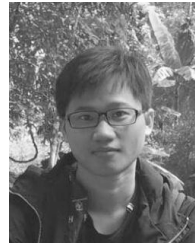
YU-MING WU was born in Zhanjiang, China, in 1992. He received the B.E. degree from the School of Information and Computer, Anhui Agricultural University, majoring in communication engineering, in 2015. He is currently pursuing the M.S. degree with the School of Electronic and Information Engineering, South China University of Technology, Guangzhou, China. His research interests are RF and microwave Antennas.

JING-YU LIN (S'14) was born in Quanzhou, China, in 1993. He received the B.S. degree in information security from Southwest Jiaotong University, Chengdu, China, in 2016. He is currently pursuing the M.S. degree from the School of Electronic and Information Engineering, South China University of Technology, Guangzhou, China.

His current research interests include cavity microwave filters and multiplexers design.

SAI-WAI WONG (S'06–M'09–SM'14) received the B.S degree in electronic engineering from The Hong Kong University of Science and Technology, Hong Kong, in 2003, and the M.Sc. and Ph.D. degrees in communication engineering from Nanyang Technological University, Singapore, in 2006 and 2009, respectively.

From 2003 to 2005, he was the Lead of the Engineering Department in mainland of China with two manufacturing companies in Hong Kong. From 2009 to 2010, he was a Research Fellow with the Institute for Infocomm Research, Singapore. In 2016, he was a Visiting Professor with the City University of Hong Kong, Hong Kong. From 2010 to 2016, he was an Associate Professor and became a Full Professor in 2016 with the School of Electronic and Information Engineering, South China University of Technology, Guangzhou, China. Since 2017, he has been a Full Professor with the College of Information, Shenzhen University, Shenzhen, China. His current research interests include RF/microwave circuit and antenna design.

Dr. Wong was a recipient of the New Century Excellent Talents in University Award in 2013. He is a Reviewer for several top-tier journals.

FEI DENG (S'15) was born in Nanchang, China, in 1992. He received the B.E. degree from Nanchang University, majoring in communication engineering, in 2015. He is currently pursuing the M.S. degree with the School of Electronic and Information Engineering, South China University of Technology, Guangzhou, China. His research interests are multiple band and tunable RF and microwave filters.

LEI ZHU (S'91–M'93–SM'00–F'12) received the B.Eng. and M.Eng. degrees in radio engineering from Southeast University, Nanjing, China, in 1985 and 1988, respectively, and the Ph.D. Degree in electronic engineering from the University of Electro-Communications, Tokyo, Japan, in 1993.

From 1993 to 1996, he was a Research Engineer with Matsushita-Kotobuki Electronics Industries Ltd., Tokyo, Japan. From 1996 to 2000, he was a Research Fellow with the Faculty of Engineering, University of Montreal, Quebec, Canada. From 2000 to 2013, he was an Associate Professor with the School of Electrical and Electronic Engineering, Nanyang Technological University, Singapore. Since 2013, he has been a Professor with the Faculty of Science and Technology, University of Macau, Macau, China, where he has been serving as the Head of the Electrical and Computer Engineering Department since 2014.

He has authored or co-authored 246 papers in peer-reviewed journals and conference proceedings, including 80 papers in the IEEE transactions/letters/magazine. His research interests include microwave circuits, antenna technique, and applied electromagnetics. His papers have been cited over 3088 times with the h-index of 31 and average citations per paper of 18.18 (source: ISI Web of Science).

Dr. Zhu has been a Member of the IEEE MTT-S Technical Committee on Computer-Aided Design since 2006, and a Member of the IEEE MTT-S Fellow Evaluation Committee since 2013. In 2011, he was elevated to the IEEE fellow for contributions to modeling, design and development of planar microwave filters. He was an Associate Editor of the IEEE Transactions on Microwave Theory and Techniques (2010–2013), an Associate Editor of the IEEE Microwave and Wireless Components Letters (2006–2012), and an Associate Editor of the *IEICE on Electronics* (2003–2005). He served as the General Chair of the 2008 IEEE MTT-S International Microwave Workshop Series on the Art of Miniaturizing RF and Microwave Passive Components, Chengdu, China, and a Technical Program Committee Co-Chair of the 2009 Asia–Pacific Microwave Conference, Singapore. He was a recipient of the 1997 Asia–Pacific Microwave Prize Award, the 1996 Silver Award of Excellent Invention from the Matsushita-Kotobuki Electronics Industries Ltd., and the 1993 First-Order Achievement Award in science and technology from the National Education Committee, China.

QING-XIN CHU (M'99–SM'11) received the B.S., M.E., and Ph.D. degrees from Xidian University, Xi'an, China, in 1982, 1987, and 1994, respectively, all in electronic engineering.

He is currently a Chair Professor with the School of Electronic and Information Engineering, South China University of Technology, where he is also the Director of the Research Institute of Antennas and RF Techniques, the chair of the Engineering Center of Antennas and RF Techniques of Guangdong Province. He has also been with Xidian University as a Distinguished Professor in Shaanxi Hundred-Talent Program since 2011. From 1982 to 2004, he was with the School of Electronic Engineering, Xidian University, and since 1997, he has been a Professor and the Vice-Dean of the School of Electronic Engineering, Xidian University.

He has authored over 300 papers in journals and conferences, which were indexed in SCI over 1500 times. One of his papers published in the IEEE Transactions on A Tntennas and P Tropagations in 2008 becomes the top Essential Science Indicators paper within ten years in the field of antenna (SCI indexed self-excluded in the antenna field ranged top 1%). He has authorized over 30 invention patents of China. He is the Foundation Chair of the IEEE Guangzhou AP/MTT Chapter, the Senior Member of the China Electronic Institute. In 2014, he was elected as the highly cited scholar by Elsevier in the field of electrical and electronic engineering.

Dr. Chu was a recipient of the Science Award by Guangdong Province in 2013, the Science Awards by the Education Ministry of China in 2008 and 2002, the Fellowship Award by the Japan Society for Promotion of Science in 2004, the Singapore Tan Chin Tuan Exchange Fellowship Award in 2003, and the Educational Award by Shaanxi Province in 2003.

His current research interests include antennas in wireless communication, microwave filters, spatial power combining array, and numerical techniques in electromagnetics.
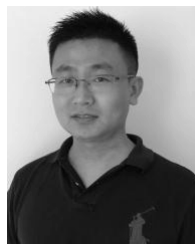
YANG YANG (S'11–M'14) received the Ph.D. degree from Monash University, Melbourne, Australia, in 2013. From 2012 to 2015, he was an Asia–Pacific GSP Engineer with Rain Bird. He served as a Senior Research Associate with the Department of Engineering, Macquarie University, from 2015 to 2016. In 2016, he was a Research Fellow with the State Key Laboratory of Millimeter-Waves, City University of Hong Kong. Since 2016, he has been the Lecturer with the University of Technology Sydney. His research interests include microwave and millimeter-wave circuits, reconfigurable antennas, wearable antennas, biosensors, and sensing technology. He was a recipient of the Global GSP Success Award in 2014.

• • •